

PAPER • OPEN ACCESS

Kinetics of individual grains during recrystallization of cold-rolled copper

To cite this article: F X Lin *et al* 2015 *IOP Conf. Ser.: Mater. Sci. Eng.* **82** 012048

View the [article online](#) for updates and enhancements.

You may also like

- [Highly alloyed Ni–W substrates for low AC loss applications](#)
Uwe Gaitzsch, Jens Hänisch, Ruben Hühne *et al.*
- [Simulation and experimental study on microstructure evolution of 5CrNiMoV steel during multi-directional non-isothermal forging](#)
Zhiqiang Hu, Kaikun Wang and Li Yang
- [Identification of texture characteristics for improved creep behavior of a L-PBF fabricated IN738 alloy through micromechanical simulations](#)
Mahesh R G Prasad, Abhishek Biswas, Napat Vajragupta *et al.*

ECS
The
Electrochemical
Society
Advancing solid state &
electrochemical science & technology

DISCOVER
how sustainability
intersects with
electrochemistry & solid
state science research

Kinetics of individual grains during recrystallization of cold-rolled copper

F X Lin¹, Y B Zhang¹, S O Poulsen², N Schell³, W Pantleon⁴ and D Juul Jensen¹

¹Danish-Chinese Center for Nanometals, Section for Materials Science and Advanced Characterization, Department of Wind Energy, Technical University of Denmark, Risø Campus, 4000 Roskilde, Denmark

²Department of Materials Science and Engineering, Northwestern University, Evanston, IL 60208-3108, USA

³Helmholtz-Zentrum Geesthacht, Institute of Materials Research, Max-Planck-Straße 1, 21502 Geesthacht, Germany

⁴Section for Materials and Surface Engineering, Department of Mechanical Engineering, Technical University of Denmark, 2800 Kongens Lyngby, Denmark
E-mail: lnfe@dtu.dk

Abstract. The formation of a recrystallization texture is closely related to the nucleation and growth of recrystallizing grains, which may vary from grain to grain. Cube texture is a commonly observed recrystallization texture in face centered cubic metals of medium to high stacking fault energy after heavy cold-rolling and annealing. In this work, recrystallization of pure copper cold-rolled to a von Mises strain of 2.7 was investigated *in situ* using three-dimensional X-ray diffraction. Growth curves of 835 grains were determined, and the curves of cube and noncube grains were compared. It was found that the nucleation times of cube grains and non-cube grains were similar, whereas the growth rates of a few but not all cube grains were high. Effects hereof for the development of the cube texture were discussed.

1. Introduction

Recrystallization kinetics and formation of a strong cube texture in heavily cold-rolled face centered cubic metals have been extensively studied both experimentally and theoretically (e.g. [1-4]). Most experimental studies of recrystallization kinetics are based on a series of partially recrystallized samples characterized by optical or electron microscopy (e.g. [5]). More recently, 3D X-ray diffraction (3DXRD) microscopy was developed and used to study recrystallization kinetics of cold-rolled aluminium [6], which showed that each recrystallizing grain followed its own kinetics. The objective of the present work is to study recrystallization kinetics of individual grains for cold-rolled copper using 3DXRD. The kinetics of cube grains and noncube grains are compared to discuss the cube texture development.

2. Experimental

The initial material was oxygen free high conductivity copper (purity 99.95%), with a grain size of 22 μm (intercept length, ignoring twin boundaries). It was cold-rolled from 5 mm to 0.5 mm, corresponding to a von Mises strain of 2.7. Recrystallization in this material has been studied by electron microscopy, and a strong cube texture is known to develop during recrystallization [7,8]. A specimen was cut from the rolled sample of ~ 2 mm along the rolling direction (RD) and 0.75 mm along the transverse direction (TD), and was electropolished to avoid nucleation from surface imperfections during the subsequent annealing.



Content from this work may be used under the terms of the [Creative Commons Attribution 3.0 licence](https://creativecommons.org/licenses/by/3.0/). Any further distribution of this work must maintain attribution to the author(s) and the title of the work, journal citation and DOI.

The 3DXRD experiment was conducted at beamline P07 at PETRA III, Deutsches Elektronen-Synchrotron (DESY) using a monochromatic X-ray beam of energy 50 keV and a square beam profile of size $500 \times 500 \mu\text{m}^2$. The specimen was mounted in a hot finger furnace with an inert gas atmosphere, with RD parallel to the vertical direction and TD parallel to the beam direction. The specimen was heated *in situ* at 130 °C, and the specimen was rotated around the vertical axis from 0° to 30° (the rotation angle was noted as ω) by sweeping a small 0.5° interval while acquiring diffraction images. Each 30° rotation took 5.7 min, and the entire measurement took about 250 min. According to hardness measurements, the sample was ~25% recrystallized at the end of the measurement.

Diffraction peaks from the {200} and {400} Debye-Scherrer rings were analyzed. The positions of diffraction peaks were identified from images collected during the last rotation. It should be noted that only peaks with relatively high peak intensities were considered. These peaks were then traced back to earlier times. Fig. 1 illustrates this process using a {200} peak as an example. Peaks were divided into two groups: originating from cube or noncube grains. A peak was considered as originating from a cube oriented grain, if the corresponding scattering vector deviated less than 10° from that of the ideal cube orientation. Since this treatment used only the partial orientation information from a single diffraction peak, cube grains in this work are actually grains with either RD or ND close to a <100> direction. However, according to EBSD data of the same sample after recrystallization [8], only very few grains (~2%) would be mislabeled; this treatment seems thus acceptable. The peak intensity was calculated as the integrated intensity over a peak subtracting its background. The intensities were converted to grain volumes as in [9], and equivalent sphere diameters (ESDs) were calculated from the obtained grain volumes. The growth curve of each grain was plotted as ESDs increasing as a function of annealing time. All growth curves were manually checked to remove artifacts.

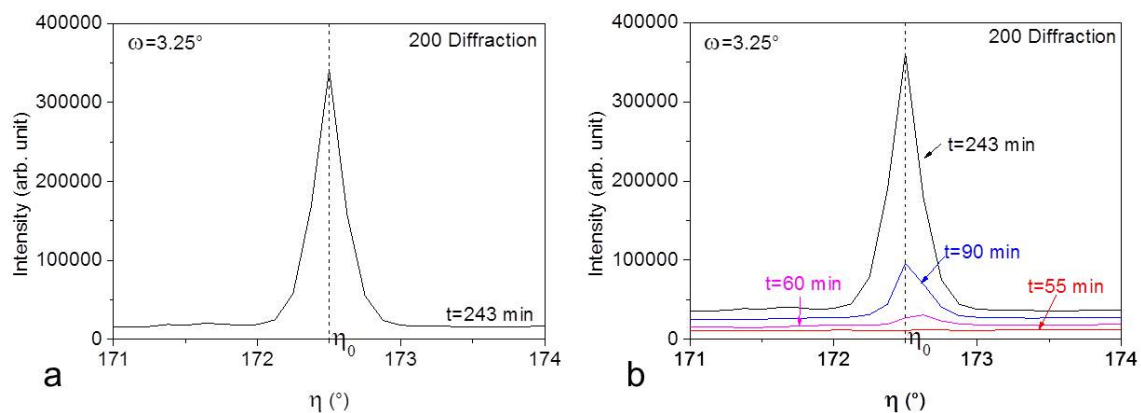


Fig. 1 Example showing the process of peak identification. a) The peak was first identified from the diffraction image collected during the last 30° rotation. The peak position (ω, η_0) were noted. b) The same peak at earlier times was found according to the peak position. This peak first appeared at $t=60$ min, and its intensity increased with time. For clarity, the peak is only plotted for a few time steps.

3. Results and discussion

In total, 101 cube grains and 724 noncube grains were identified in the last time step. The grain size (ESD) distributions are plotted in Fig. 2. Compared with noncube grains, cube grains have a higher fraction of grains smaller than 10 μm . All these small cube grains have peak positions near the azimuthal angles 0° or 180°. These peak intensities are thus enhanced by the Lorentz factor. It means that the detection limit (minimum grain size) is smaller for cube grains. To avoid this bias, all grains smaller than 10 μm are excluded in the following analysis. As shown by Fig. 2, the size distribution of noncube grains is observed to follow a lognormal distribution, but that of cube grains is not. There are a certain number of cube grains larger than 40 μm , and the largest cube grain is 88 μm . The size distribution of

cube grains is consistent with previous observations using electron backscatter diffraction in the same material after annealing at 150 °C [8]. The large cube grains have been termed supercube grains [8], and although few in number, these supercube grains make a significant contribution to the cube texture.

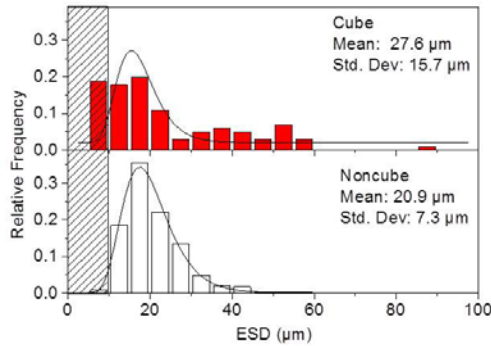


Fig. 2 Size distributions of cube and noncube grains at the end of the measurement (~25% recrystallized). There are more cube grains smaller than 10 μm, because of the different detection limits for cube and noncube grains (see text in Section 3 for details). To avoid this bias, a cut-off size of 10 μm was used, i.e. grains in the shaded part are not included in the following analysis. The size distributions of grains larger than 10 μm were fitted to lognormal functions.

A few typical growth curves are plotted in Fig. 3. Each grain follows its own growth curve, as has been observed for aluminium [6]. The growth rates vary with time and from grain to grain. Most grains tend to have a large growth rate right after nucleation, followed by a period during which the growth rate decreases. A few grains, such as the one marked by an arrow in Fig. 3a, exhibit a stagnation period for some time, after which they continue to grow. The nucleation times vary significantly from grain to grain, which is different from aluminium [6]. To compare the nucleation and growth behavior of cube and noncube grains, we obtained two parameters from each growth curve: the nucleation time t_n and the maximal growth rate g . Fig. 3b illustrates how the two parameters were obtained.

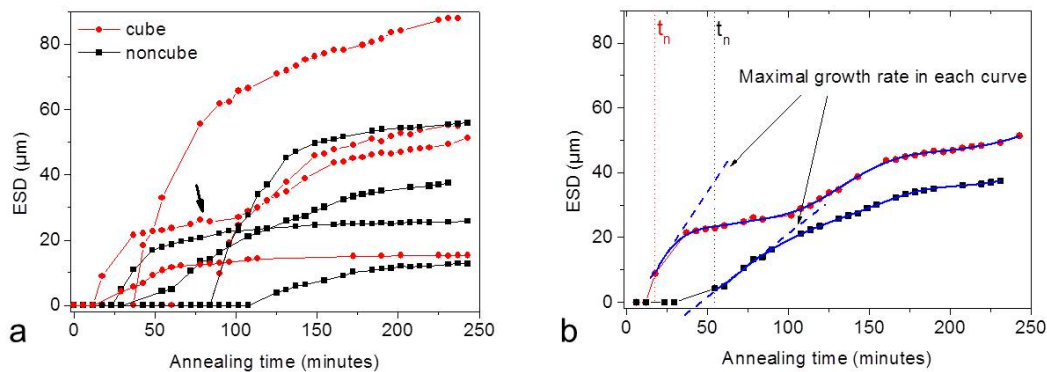


Fig. 3 Selection of measured growth curves. a) Growth curves of 4 cube grains and 4 noncube grains. The arrow marks a stagnation period. b) Examples explaining how the nucleation time t_n and maximal growth rates g were determined. t_n was the time when the grain was first observed. Each growth curve was fitted using a spline function (the blue curve), and the largest slope of the fitted curve was used as g .

The distributions of the nucleation times are plotted in Fig. 4a. Nucleation takes place during the entire measurement period for both cube and noncube grains. There is a slightly higher fraction of cube grains that nucleate during the first 30 min (see the first bin of the histograms in Fig. 4a), but according to the cumulative relative frequency, the nucleation behavior of cube and noncube grains is considered quite similar. Therefore, the different size distributions seem not to be associated with differences in the nucleation times.

The distributions of the maximal growth rates are plotted in Fig. 4b. For most cube and noncube grains, the maximal growth rates are less than 0.4 μm/min, but cube grains have more grains with higher growth rates. This tendency is clearer from the cumulative relative frequencies: the 70% slowest growing grains have similar maximal growth rates for both cube

and noncube grains, whereas the 30% fastest growing cube grains show a significantly enhanced growth rate than the 30% fastest growing noncube grains. The few cube grains with larger growth rates may grow to larger grain sizes, which explains the longer tail in the size distribution of cube grains, i.e. the formation of supercube grains. However, as the growth rate of one grain varies with time, it is insufficient to use only the maximal growth rate in a growth curve to represent the growth behavior of a grain. We are planning to include more parameters to compare the growth behavior of cube and noncube grains in the future.

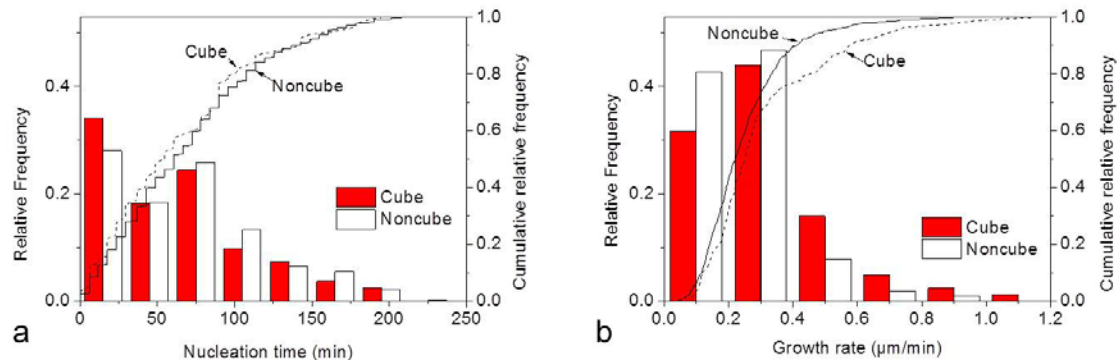


Fig. 4 Distributions of nucleation times t_n (a) and maximal growth rates g (b) for cube and noncube grains that are larger than $10 \mu\text{m}$ at the end of the measurement. The histograms show the relative frequencies, and the curves show the cumulative relative frequencies. The bin widths are 30 min and $0.2 \mu\text{m}/\text{min}$ for a) and b) respectively.

4. Summary

Nucleation and growth of individual grains in cold-rolled copper have been followed *in situ* during recrystallization at $130 \text{ }^\circ\text{C}$ by 3DXRD. A few cube grains having large sizes after recrystallization, named supercube grains, are important for the cube texture development. Cube and noncube grains seem to have similar nucleation behavior but different growth rates. More cube grains have larger growth rates, and this is considered to be related to the formation of the supercube grains.

Acknowledgements

The authors gratefully acknowledge the support from the Danish National Research Foundation (Grant No. DNRF86-5) and the National Natural Science Foundation of China (Grant No. 51261130091) for the Danish-Chinese Center for Nanometals, within which this work was performed. The authors also acknowledge beamtime by DESY under proposal number I-20110560 EC. We would like to thank Torben Fischer and Lars Lottermoser for assistance in using beamline P07.

References

- [1] Vandermeer R A and Juul Jensen D 1995 *Metall. Mater. Trans. A* **26** 2227
- [2] Juul Jensen D 1997 *Metall. Mater. Trans. A* **28** 15
- [3] Wassermann G and Grewen J 1962 *Texturen metallischer Werkstoffe* Springer-Verlag Berlin pp 307-326
- [4] Necker C T et al. 1991 *Texture. Microstruct.* **14-18** 635
- [5] Vandermeer R A and Gordon P 1989 *Metal. Trans. A* **20** 391
- [6] Lauridsen E M et al. 2003 *Acta Mater.* **51** 4423
- [7] Lin F X et al. 2012 *Mater. Sci. Forum* **702-703** 398
- [8] Lin F X et al. *To be submitted*
- [9] Poulsen S O et al. 2011 *Scr. Mater.* **64** 1003